Soomin Choi
Graduate Research Assistant
School of Mechanical
and Aerospace Engineering,
Seoul National University,
Shinlim-Dong, San 56-1,
Kwanak-Gu, Seoul 151-742, Korea
e-mail: soomin0603@snu.ac.kr

Gang-Won Jang
Associate Professor
Faculty of Mechanical
and Aerospace Engineering,
Sejong University,
98 Gunja-Dong, Gwangjin-Gu
Seoul 143-747, Korea
e-mail: gwjang@sejong.ac.kr

Yoon Young Kim[1]
Professor
WCU Multiscale Mechanical Design Division,
School of Mechanical
and Aerospace Engineering,
Seoul National University,
Shinlim-Dong, San 56-1, Kwanak-Gu,
Seoul 151-742, Korea
e-mail: yykim@snu.ac.kr

Exact Matching Condition at a Joint of Thin-Walled Box Beams Under Out-of-Plane Bending and Torsion

To take into account the flexibility resulting from sectional deformations of a thin-walled box beam, higher-order beam theories considering warping and distortional degrees of freedom (DOF) in addition to the Timoshenko kinematic degrees have been developed. The objective of this study is to derive the exact matching condition consistent with a 5-DOF higher-order beam theory at a joint of thin-walled box beams under out-of-plane bending and torsion. Here we use bending deflection, bending/shear rotation, torsional rotation, warping, and distortion as the kinematic variables. Because the theory involves warping and distortion that do not produce any force/moment resultant, the joint matching condition cannot be obtained just by using the typical three equilibrium conditions. This difficulty poses considerable challenges because all elements of the 5×5 transformation matrix relating the field variables of one beam to those in another beam should be determined. The main contributions of the investigation are to propose additional necessary conditions to determine the matrix and to derive it exactly. The validity of the derived joint matching transformation matrix is demonstrated by showing good agreement between the shell finite element results and those obtained by the present box beam analysis in various angle box beams. [DOI: 10.1115/1.4006383]

Keywords: thin-walled box beam, warping, distortion, angled joint, joint matching condition, out-of-plane bending, torsion, transformation matrix

1 Introduction

This work is concerned with the analysis of thin-walled box beams connected through angled joints under out-of-plane bending and torsion as depicted in Fig. 1. The analysis will be carried out by higher-order beam theories that employ five kinematic variables representing sectional warping (U) and distortion (χ) in addition to the standard Timoshenko kinematic variables such as vertical bending deflection (V), bending/shear rotation (β), and torsional rotation (θ). The displacements or deformations of the cross section of a box beam corresponding to the five kinematic variables are illustrated in Fig. 2. The importance of considering warping and distortion in thin-walled closed beams has been addressed in earlier investigations [1–9] and several forms of higher-order theories have been developed for straight box beams [1,3,5,8,10,11].

Nevertheless, there is no box beam theory based theoretical method to exactly match the degrees of freedom at an angle joint where two straight box beams are connected. The significant local effects appearing near joints of thin-walled box beams have been pointed out in several investigations [12–16]. The joint-related investigations using a higher-order beam theory were first given by Jang et al. [17–19], but the approach used an approximate technique that minimizes the difference between three-dimensional displacements in the sections of two beams connected at an angled joint. On the contrary, we aim to derive the *exact* condition relating the field variables of one box beam to those of another box beam at the joint using a higher-order beam theory.

In deriving the joint matching condition, we will employ the higher-order beam theory given in [17] which employs the above-mentioned five field variables. The joint matching condition can be expressed by a 5×5 transformation matrix $\mathbf{T}(\phi)$ (ϕ: joint angle) relating $\mathbf{U}_1$ and $\mathbf{U}_2$ as $\mathbf{U}_2 = \mathbf{T}(\phi)\mathbf{U}_1$, where $\mathbf{U}_p = \{V, \beta, \theta, U, \chi\}_p^{\mathrm{T}} (p = 1, 2)$ is the field variable vector of beam p. For a later use, we introduce the symbol $\mathbf{F}_p = \{P, M, H, B, Q\}_p^{\mathrm{T}}$ to denote the generalized force vector, which is the work conjugate of $\mathbf{U}_p$. Here, P, M, and H denote vertical shear force, bending moment, and twisting moment, respectively. Note that they all have resultants. On the other hand, the bimoment B and transverse bimoment Q have no resultant, i.e., they represent self-equilibrated terms. In case of the Euler or Timoshenko beam, a 3×3 transformation matrix involving only $\{V, \beta, \theta\}$ can be derived only by considering equilibrium conditions. Since warping and distortion that are self-equilibrated deformations are also used in a thin-walled box beam theory, however, additional conditions must be used. To derive all components of the 5×5 $\mathbf{T}$ matrix, we propose to consider the following three additional conditions in addition to the equilibrium conditions.

(1) Because B_1 and Q_1 have no resultant, P_2, M_2, and H_2 should not be coupled with B_1 and Q_1 at the joint of two box beams.
(2) At the so-called intersection points of two box beams at an angled joint, the three-dimensional displacements should be continuous.
(3) A fundamental transformation rule $\mathbf{T}(\phi) \cdot \mathbf{T}(-\phi) = \mathbf{I}$ ($\mathbf{I}$: identity matrix) must be satisfied for any value of ϕ.
(4) Another fundamental transformation identity $\mathbf{T}(\phi) \cdot \mathbf{T}(\phi) = \mathbf{T}(2\phi)$ must hold. Conditions (3) and (4) seem to be trivial, but they play critical roles in determine all 5×5 elements exactly.

To check the validity of the derived transformation matrix $\mathbf{T}(\phi)$, two case problems will be examined. Because the problems to be considered were also solved by an approximate method, the accuracy by the present exact condition may be better demonstrated. The converged finite element results obtained with the ANSYS shell elements [20] will be used as the reference results.

2 Higher-Order Beam Theory for Straight Box Beams

A higher-order beam theory for a rectangular box beam in [10,17] will briefly explained as a basis for all subsequent

[1]Corresponding author.

Manuscript received August 30, 2011; final manuscript received January 21, 2012; accepted manuscript posted March 15, 2012; published online June 28, 2012. Assoc. Editor: Daining Fang.

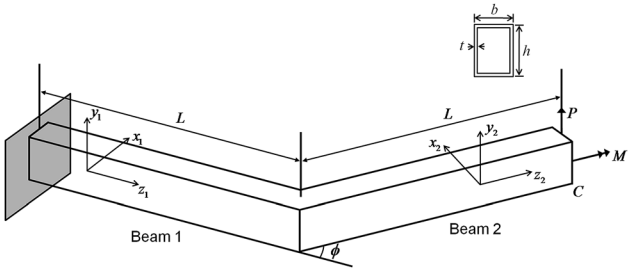

Fig. 1 Thin-walled box beams connected at an angled joint

analyses. As depicted in Fig. 2, each edge has its own coordinate (n, s); the tangential coordinate s is measured along the contour (or center line) of the wall starting from the center, and the normal coordinate n is measured by the outward normal distance from the contour. The three-dimensional displacements of a point on the contour can be expressed in terms of the five one-dimensional field variables, $\mathbf{U} = \{V, \beta, \theta, U, \chi\}^{\mathrm{T}}$, as

$$u_n(s,z) = \psi_n^V(s)V(z) + \psi_n^\beta(s)\beta(z) + \psi_n^\theta(s)\theta(z) + \psi_n^U(s)U(z) + \psi_n^\chi(s)\chi(z) \quad (1a)$$

$$u_s(s,z) = \psi_s^V(s)V(z) + \psi_s^\beta(s)\beta(z) + \psi_s^\theta(s)\theta(z) + \psi_s^U(s)U(z) + \psi_s^\chi(s)\chi(z) \quad (1b)$$

$$u_z(s,z) = \psi_z^V(s)V(z) + \psi_z^\beta(s)\beta(z) + \psi_z^\theta(s)\theta(z) + \psi_z^U(s)U(z) + \psi_z^\chi(s)\chi(z) \quad (1c)$$

where z is the axial coordinate, and u_s, u_n, and u_z are the tangential, normal, and axial displacements of the point on the contour, respectively. In Eq. (1), $\psi_i^\alpha(s)(i = n, s, z;\ \alpha = V, \beta, \theta, U, \chi)$ represent the deformation of the cross section along the i coordinate corresponding to the unit magnitude of field variable α. The explicit expressions of $\psi_i^\alpha(s)$ are given in the Appendix.

The three-dimensional displacements of a generic point located away from the contour by n on the cross section $\{\tilde{u}_n, \tilde{u}_s, \tilde{u}_z\}$ can be written as

$$\tilde{u}_n(n,s,z) = u_n(s,z) = \psi_n^V(s)V(z) + \psi_n^\theta(s)\theta(z) + \psi_n^\chi(s)\chi(z) \quad (2a)$$

$$\tilde{u}_s(n,s,z) = u_s(s,z) - n\frac{du_n(s,z)}{ds} = \psi_s^V(s)V(z) + \psi_s^\theta(s)\theta(z) + \psi_s^\chi(s)\chi(z) - n\frac{d\psi_n^\chi(s)}{ds}\chi(z) \quad (2b)$$

$$\tilde{u}_z(n,s,z) = u_z(s,z) = \psi_z^\beta(s)\beta(z) + \psi_z^U(s)U(z) \quad (2c)$$

where the term $(-n\,du_n(s,z)/ds)$ in Eq. (2*b*) is needed to consider the bending effect of the cross-section wall.

One can derive the expressions for the dominant components of strain from $\{\varepsilon_{ss}, \varepsilon_{sz}, \varepsilon_{zz}\}$ Eq. (2*a*) and stress $\{\sigma_{ss}, \sigma_{sz}, \sigma_{zz}\}$ by using constitutive relation. Then, from the principle of minimum potential energy, one can derive the governing equations for $V, \beta, \theta, U,$ and χ (see [10,17] for the explicit forms of equations) and also define the work conjugates of the field variables $\mathbf{F} = \{P, M, H, B, Q\}^{\mathrm{T}}$:

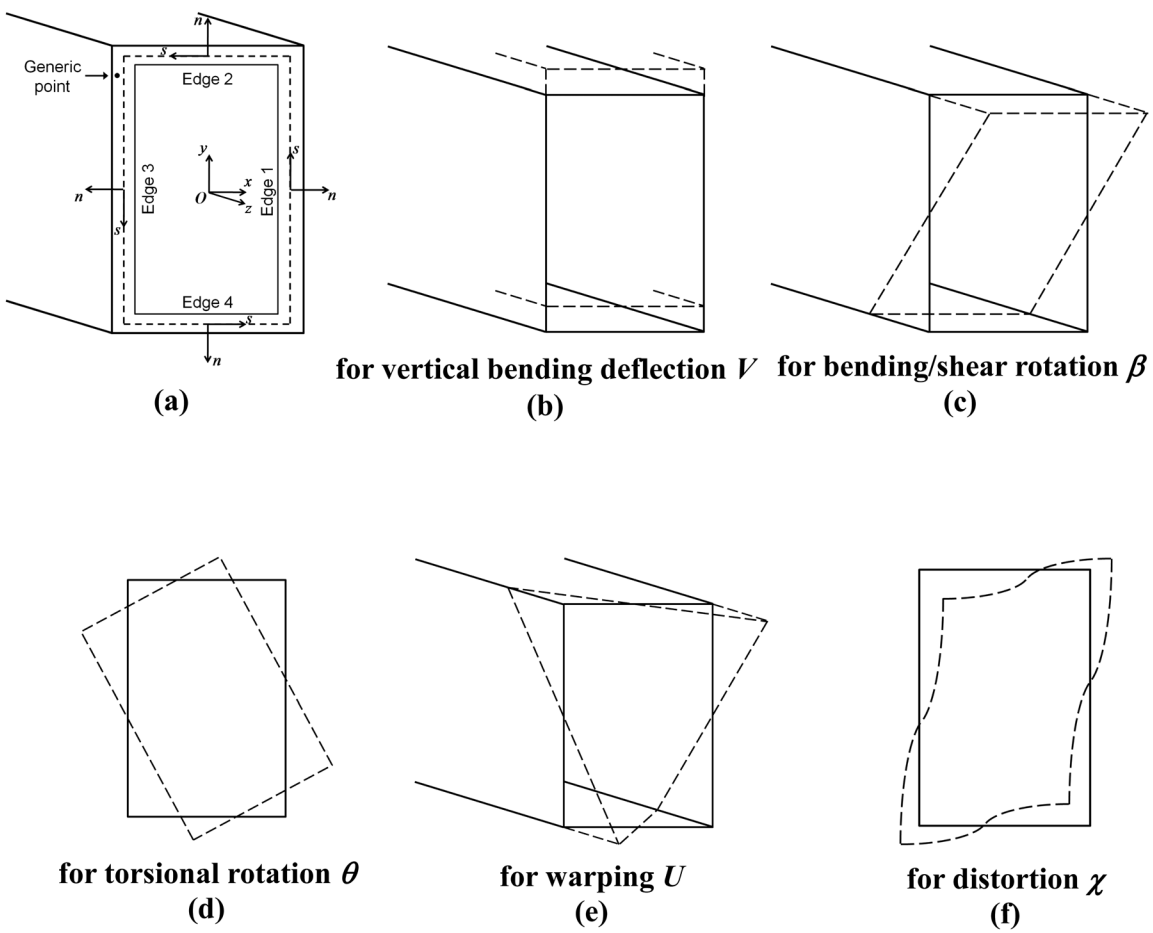

Fig. 2 (*a*) Coordinate system and (*b*)–(*f*) displacements/deformations of the beam section corresponding to the field variables (*V, β, θ, U, χ*)

$$P = \int_A \sigma_{zs}\psi_s^V dA, M = \int_A \sigma_{zz}\psi_z^\beta dA, H = \int_A \sigma_{zs}\psi_s^\theta dA,$$
$$B = \int_A \sigma_{zz}\psi_z^U dA, Q = \int_A \sigma_{zs}\psi_s^\chi dA \tag{3}$$

As defined in the Introduction $P, M, H, B,$ and Q denote the one-dimensional force measures representing vertical force, bending moment, twisting moment, bimoment, and transverse bimoment, respectively.

3 Derivation of the Exact Joint Matching Condition

Thin-walled box beams (indicated by beam 1 and beam 2 in Fig. 1) meet each other at an angle of ϕ in the x-z plane. The relation between the field variable vector $\mathbf{U}_1$ of beam 1 and $\mathbf{U}_2$ of beam 2 may be expressed in terms of a transformation matrix $\mathbf{T}(\phi)$ such that

$$\mathbf{U}_2 = \mathbf{T}(\phi)\mathbf{U}_1 \tag{4a}$$

or

$$\begin{Bmatrix} V \\ \beta \\ \theta \\ U \\ \chi \end{Bmatrix}_2 = \begin{bmatrix} t_{11} & t_{12} & t_{13} & t_{14} & t_{15} \\ t_{21} & t_{22} & t_{23} & t_{24} & t_{25} \\ t_{31} & t_{32} & t_{33} & t_{34} & t_{35} \\ t_{41} & t_{42} & t_{43} & t_{44} & t_{45} \\ t_{51} & t_{52} & t_{53} & t_{54} & t_{55} \end{bmatrix} \begin{Bmatrix} V \\ \beta \\ \theta \\ U \\ \chi \end{Bmatrix}_1 \tag{4b}$$

The matrix $\mathbf{T}$ depends not only on ϕ but also on the box beam geometry (such as b (width), h (height), and t (thickness) defined in Fig. 1), but it will be simply written as $\mathbf{T}(\phi)$ to emphasize its dependence on ϕ.

Before using the four propositions given at the end of the Introduction, we first recall the well-known relation. If $\mathbf{U}_2$ and $\mathbf{U}_1$ are related by $\mathbf{T}(\phi)$ by Eq. (4a), $\mathbf{F}_2$ and $\mathbf{F}_1$ are related as

$$\mathbf{F}_2 = \mathbf{T}^*\mathbf{F}_1 = \mathbf{T}^{-\mathrm{T}}(\phi)\mathbf{F}_1 \tag{5}$$

Equation (5) is the direct consequence of the virtual work conservation at the joint such that

$$\mathbf{F}_1^{\mathrm{T}}\delta\mathbf{U}_1 = \mathbf{F}_2^{\mathrm{T}}\delta\mathbf{U}_2 \tag{6}$$

where $\delta\mathbf{U}_p$ denotes the variation of $\mathbf{U}_p (p = 1, 2)$.

Another well-known relation is the force/moment equilibrium at a joint:

$$\begin{Bmatrix} P \\ M \\ H \end{Bmatrix}_2 = \begin{bmatrix} 1 & 0 & 0 \\ 0 & \cos\phi & -\sin\phi \\ 0 & \sin\phi & \cos\phi \end{bmatrix} \begin{Bmatrix} P \\ M \\ H \end{Bmatrix}_1 \tag{7}$$

Because B and Q represent self-equilibrated bimoments, they do not appear in the equilibrium relation, Eq. (7). Now let us consider the four conditions proposed in the Introduction to determine all of the 5×5 components of $\mathbf{T}(\phi)$.

3.1 Proposition 1: Consideration of No Resultant by B and Q.

First of all, we observe that torsional (B) and transverse (Q) bimoments are in a state of self-equilibrium. This observation implies that the generalized force terms (P_2, M_2, H_2) in beam 2 should not be affected by the self-equilibrated force terms (B_1, Q_1) of beam 1. Therefore, the relations between $\mathbf{F}_1$ and $\mathbf{F}_2$ should be written as

$$\begin{Bmatrix} P \\ M \\ H \\ B \\ Q \end{Bmatrix}_2 = \left[\begin{array}{ccc:cc} 1 & 0 & 0 & 0 & 0 \\ 0 & \cos\phi & -\sin\phi & 0 & 0 \\ 0 & \sin\phi & \cos\phi & 0 & 0 \\ \hdashline \bullet & \bullet & \bullet & \bullet & \bullet \\ \bullet & \bullet & \bullet & \bullet & \bullet \end{array}\right] \begin{Bmatrix} P \\ M \\ H \\ B \\ Q \end{Bmatrix}_1 \tag{8}$$

In Eq. (8), the zeros appearing inside the dotted rectangle are the consequences of the above-mentioned observation while 10 solid circles represent the elements to be determined. Noting that the transformation matrix appearing in Eq. (8) is $\mathbf{T}^*$, which is equal to $\mathbf{T}^{-\mathrm{T}}$ by Eq. (5), one can show that the matrix $\mathbf{T}$ must take the following form;

$$\mathbf{T} = \begin{bmatrix} 1 & 0 & 0 & t_{14} & t_{15} \\ 0 & \cos\phi & -\sin\phi & t_{24} & t_{25} \\ 0 & \sin\phi & \cos\phi & t_{34} & t_{35} \\ 0 & 0 & 0 & t_{44} & t_{45} \\ 0 & 0 & 0 & t_{54} & t_{55} \end{bmatrix} \tag{9}$$

where the 10 components of that the matrix $\mathbf{T}(t_{14}, t_{15}, \ldots, t_{55})$ are the quantities that cannot be determined from the equilibrium consideration.

3.2 Proposition 2: Three-Dimensional Displacement Continuity at the Intersection Points.

In theory, the three-dimensional displacements at every point of the common interfacing region of beams 1 and 2 should be continuous. However, it is not possible to strictly impose the continuity condition because only a finite number of one-dimensional field variables are used in the box beam theory. To use the one-dimensional beam theory for the joint, let us consider the top view of the connected beams in the x-z plane in Fig. 3(a). Here, two beams are assumed to penetrate each other so that the centers of the cross sections of the two beams meet at point A. From the three-dimensional view of the cross sections shown in Fig. 3(b), in fact, two beams meet at A and B. Note that points A and B lie on edge 2 and 4 of the contours (center lines) of two beam cross sections, respectively.

Let us now consider the three-dimensional continuity at A:

$$(\tilde{u}_n\underset{\sim}{e}_n + \tilde{u}_s\underset{\sim}{e}_s + \tilde{u}_z\underset{\sim}{e}_z)_{\mathrm{Beam1}} = (\tilde{u}_n\underset{\sim}{e}_n + \tilde{u}_s\underset{\sim}{e}_s + \tilde{u}_z\underset{\sim}{e}_z)_{\mathrm{Beam2}} \tag{10}$$

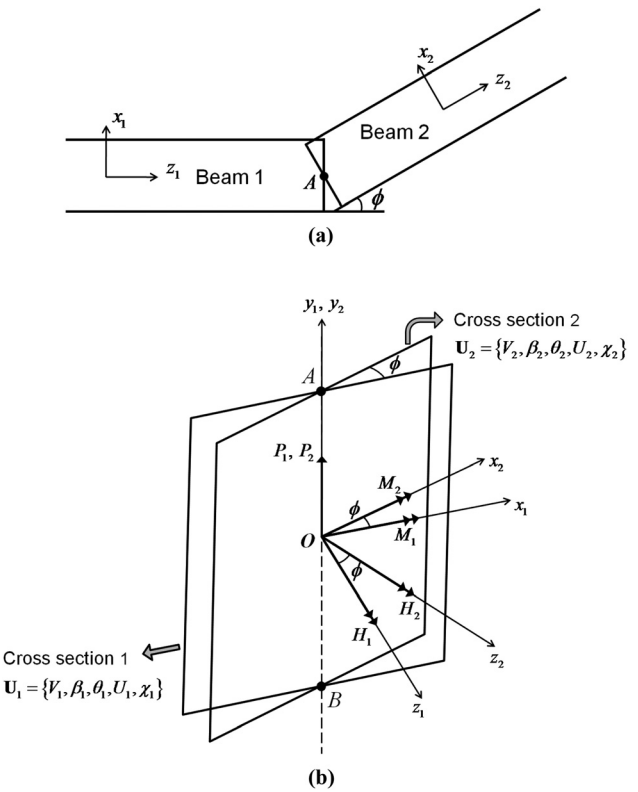

Fig. 3 (*a*) The top view of the beam centerlines in the *x-z* plane with an indication of the assumed common intersection point *A* and (*b*) beam cross sections passing though the common intersection points *A* and *B*. (The generalized force quantities having nonzero resultants are shown.)

where $\underset{\sim}{e}_q$ is the unit base vector along the local coordinate axis $q(q = n, s, z)$. Using the relation between $\underset{\sim}{e}_q|_{\text{Beam1}}$ and $\underset{\sim}{e}_q|_{\text{Beam2}}$ (see Fig. 3(*b*))

$$\underset{\sim}{e}_n|_{\text{Beam1}} = \underset{\sim}{e}_n|_{\text{Beam2}} \tag{11a}$$

$$\underset{\sim}{e}_s|_{\text{Beam1}} = \underset{\sim}{e}_s|_{\text{Beam2}} \cos\phi - \underset{\sim}{e}_z|_{\text{Beam2}} \sin\phi \tag{11b}$$

$$\underset{\sim}{e}_z|_{\text{Beam1}} = \underset{\sim}{e}_s|_{\text{Beam2}} \sin\phi + \underset{\sim}{e}_z|_{\text{Beam2}} \cos\phi \tag{11c}$$

the displacement components of beams 1 and 2 are related at A as

$$\tilde{u}_n|_{\text{Beam2}} = \tilde{u}_n|_{\text{Beam1}} \tag{12a}$$

$$\tilde{u}_s|_{\text{Beam2}} = \tilde{u}_s|_{\text{Beam1}} \cos\phi + \tilde{u}_z|_{\text{Beam1}} \sin\phi \tag{12b}$$

$$\tilde{u}_z|_{\text{Beam2}} = -\tilde{u}_s|_{\text{Beam1}} \sin\phi + \tilde{u}_z|_{\text{Beam1}} \cos\phi \tag{12c}$$

To find the relations between $\mathbf{U}_1$ and $\mathbf{U}_2$ from Eq. (12), Eq. (2) and the formula in the Appendix are used to calculate the displacement components at point A of beams 1 and 2:

$$\text{Point A}|_{\text{Beam1}} : \tilde{u}_n = V_1, \quad \tilde{u}_s = \frac{h}{2}\theta_1 - \frac{bh}{b+h}\chi_1, \quad \tilde{u}_z = \frac{h}{2}\beta_1 \tag{13}$$

$$\text{Point A}|_{\text{Beam2}} : \tilde{u}_n = V_2, \quad \tilde{u}_s = \frac{h}{2}\theta_2 - \frac{bh}{b+h}\chi_2, \quad \tilde{u}_z = \frac{h}{2}\beta_2 \tag{14}$$

Substituting Eqs. (13) and (14) into Eq. (12) and using Eq. (4) with $\mathbf{T}$ in Eq. (9) yield

$$V_2 = V_1 \tag{15}$$

$$t_{24} = 0, \quad t_{25} = \frac{2b}{b+h}\sin\phi \tag{16}$$

$$t_{34} = \frac{2b}{b+h}t_{54}, \quad t_{35} = \frac{2b}{b+h}(t_{55} - \cos\phi) \tag{17}$$

Inserting the results in Eqs. (15)–(17) into $\mathbf{T}(\phi)$ in Eq. (9) gives

$$\mathbf{T}(\phi) = \begin{bmatrix} 1 & 0 & 0 & 0 & 0 \\ 0 & \cos\phi & -\sin\phi & 0 & \frac{2b}{b+h}\sin\phi \\ 0 & \sin\phi & \cos\phi & \frac{2b}{b+h}t_{54} & \frac{2b}{b+h}(t_{55} - \cos\phi) \\ 0 & 0 & 0 & t_{44} & t_{45} \\ 0 & 0 & 0 & t_{54} & t_{55} \end{bmatrix} \tag{18}$$

Now $\mathbf{T}(\phi)$ has only four undetermined components: t_{44}, t_{45}, t_{54}, and t_{55}.

3.3 Proposition 3: Use of the Relation $\mathbf{T}(\phi) \cdot \mathbf{T}(-\phi) = \mathbf{I}$. Here we use a fundamental relation $\mathbf{T}(\phi) \cdot \mathbf{T}(-\phi) = \mathbf{I}$, where $\mathbf{I}$ is an identity matrix. To find $T(-\phi)$, the schematic figures shown in Fig. 4 will be used. Figure 4(*a*) shows two beams connected at a positive angle of ϕ while the first figure in Fig. 4(*b*) sketches two beams connected at a negative angle $-\phi$. As indicated in Fig. 4(*b*), the two beams connected at a negative angle may be viewed as two beams connected at a positive angle of ϕ in a rotated coordinate system $(\tilde{x}, \tilde{y}, \tilde{z})$ by 180 deg from the (x, y, z) coordinate system such that

$$\tilde{x} = -x, \quad \tilde{y} = -y, \quad \text{and} \quad \tilde{z} = z \tag{19}$$

If the field quantities defined in the $(\tilde{x}, \tilde{y}, \tilde{z})$ coordinate system are denoted by $\tilde{\mathbf{U}} = \{\tilde{V}, \tilde{\beta}, \tilde{\theta}, \tilde{U}, \tilde{\chi}\}^{\mathrm{T}}$, the relation between $\tilde{\mathbf{U}}_1$ and $\tilde{\mathbf{U}}_2$ is given by

$$\tilde{\mathbf{U}}_2 = \mathbf{T}(\phi)\tilde{\mathbf{U}}_1 \tag{20}$$

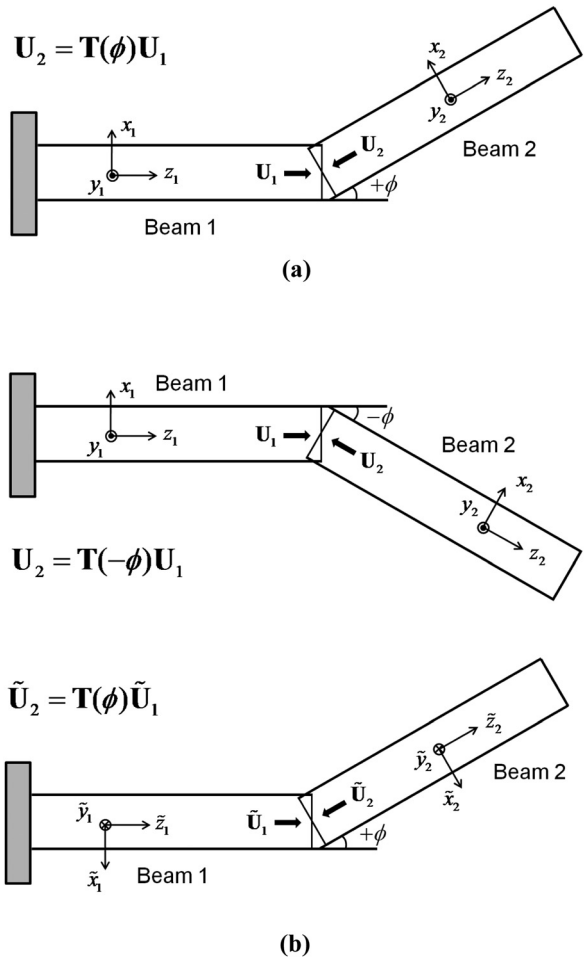

Fig. 4 Description of the procedure to obtain $\mathbf{T}(-\phi)$: (*a*) $\mathbf{T}(\phi)$ relation for a positive ϕ and (*b*) $\mathbf{T}(-\phi)$ defined for a negative ϕ, which can be derived from $\mathbf{T}(\phi)$ defined in a different coordinate system

By examining the section displacements or deformations shown in Figs. 2(*b*) –2(*f*), one can show that

$$\tilde{V} = -V, \quad \tilde{\beta} = -\beta, \quad \tilde{\theta} = \theta, \quad \tilde{W} = W, \quad \tilde{\chi} = \chi \tag{21}$$

To find the last two relations in Eq. (21), one must note that the deformation patterns of W and χ shown in Figs. 2(*e*) and 2(*f*) under the rotation produce the same deformation patterns, resulting in $\tilde{W} = W$ and $\tilde{\chi} = \chi$. Substituting Eq. (21) into Eq. (20) and doing some algebra to write Eq. (20) as $\mathbf{U}_2 = \mathbf{T}(-\phi)\mathbf{U}_1$, where $U = \{+V, +\beta, \theta, U, \chi\}^{\mathrm{T}}$, one can identify $\mathbf{T}(-\phi)$ as

$$\mathbf{T}(-\phi) = \begin{bmatrix} 1 & 0 & 0 & 0 & 0 \\ 0 & \cos\phi & \sin\phi & -t_{24} & -t_{25} \\ 0 & -\sin\phi & \cos\phi & t_{34} & t_{35} \\ 0 & 0 & 0 & t_{44} & t_{45} \\ 0 & 0 & 0 & t_{54} & t_{55} \end{bmatrix}$$

$$= \begin{bmatrix} 1 & 0 & 0 & 0 & 0 \\ 0 & \cos\phi & \sin\phi & 0 & -\frac{2b}{b+h}\sin\phi \\ 0 & -\sin\phi & \cos\phi & \frac{2b}{b+h}t_{54} & \frac{2b}{b+h}(t_{55} - \cos\phi) \\ 0 & 0 & 0 & t_{44} & t_{45} \\ 0 & 0 & 0 & t_{54} & t_{55} \end{bmatrix} \tag{22}$$

To use the fundamental transformation relation of $\mathbf{T}(\phi) \cdot \mathbf{T}(-\phi) = \mathbf{I}$, we multiply $\mathbf{T}(\phi)$ in Eq. (18) and $\mathbf{T}(-\phi)$ in Eq. (22):

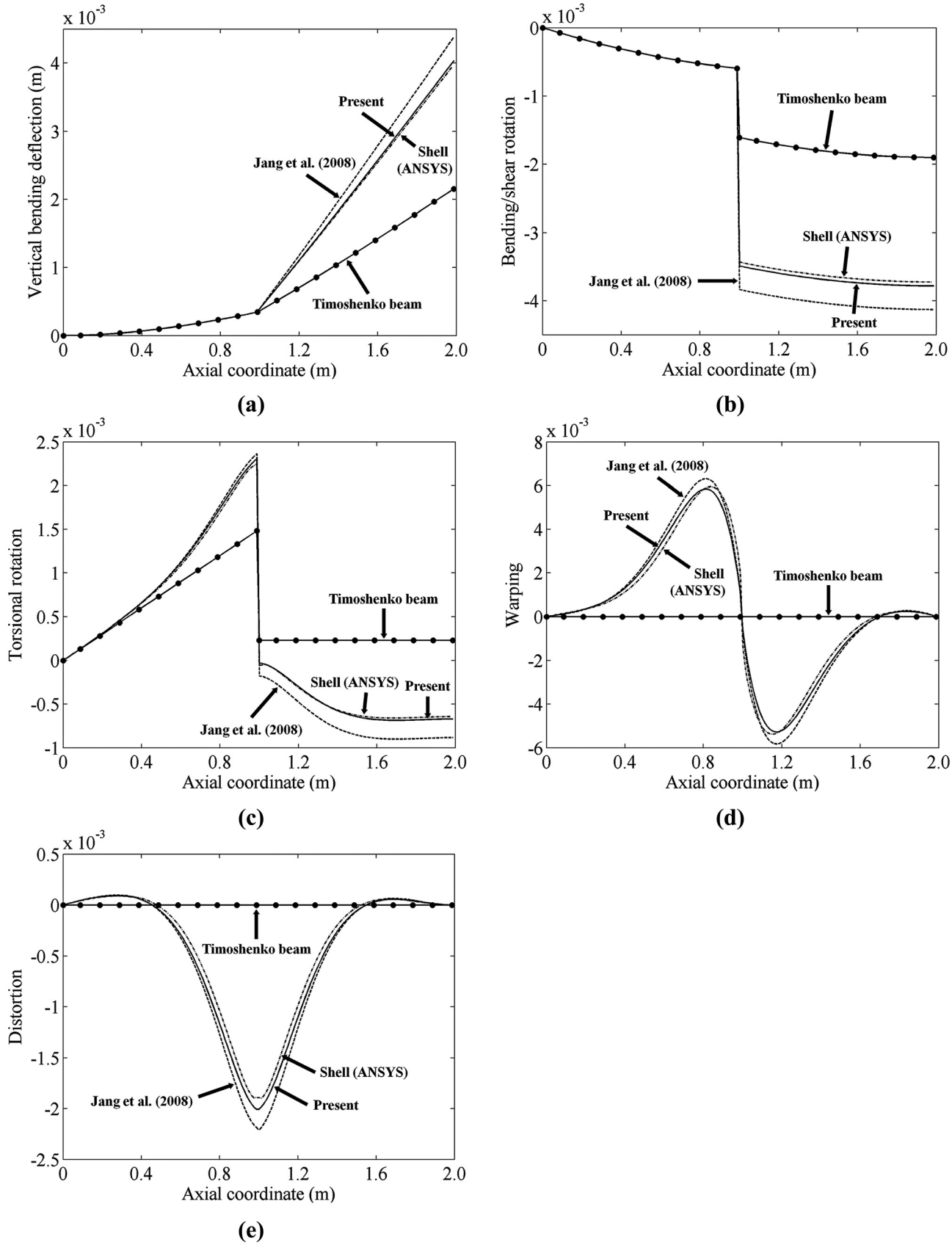

Fig. 5 Numerical results for the two-beam structure in Fig. 1 with $b = 50$ mm, $h = 100$ mm, $\phi = 60$ deg: (*a*) vertical bending deflection *V*, (*b*) bending/shear rotation β, (*c*) torsional rotation θ, (*d*) warping *U*, and (*e*) distortion χ

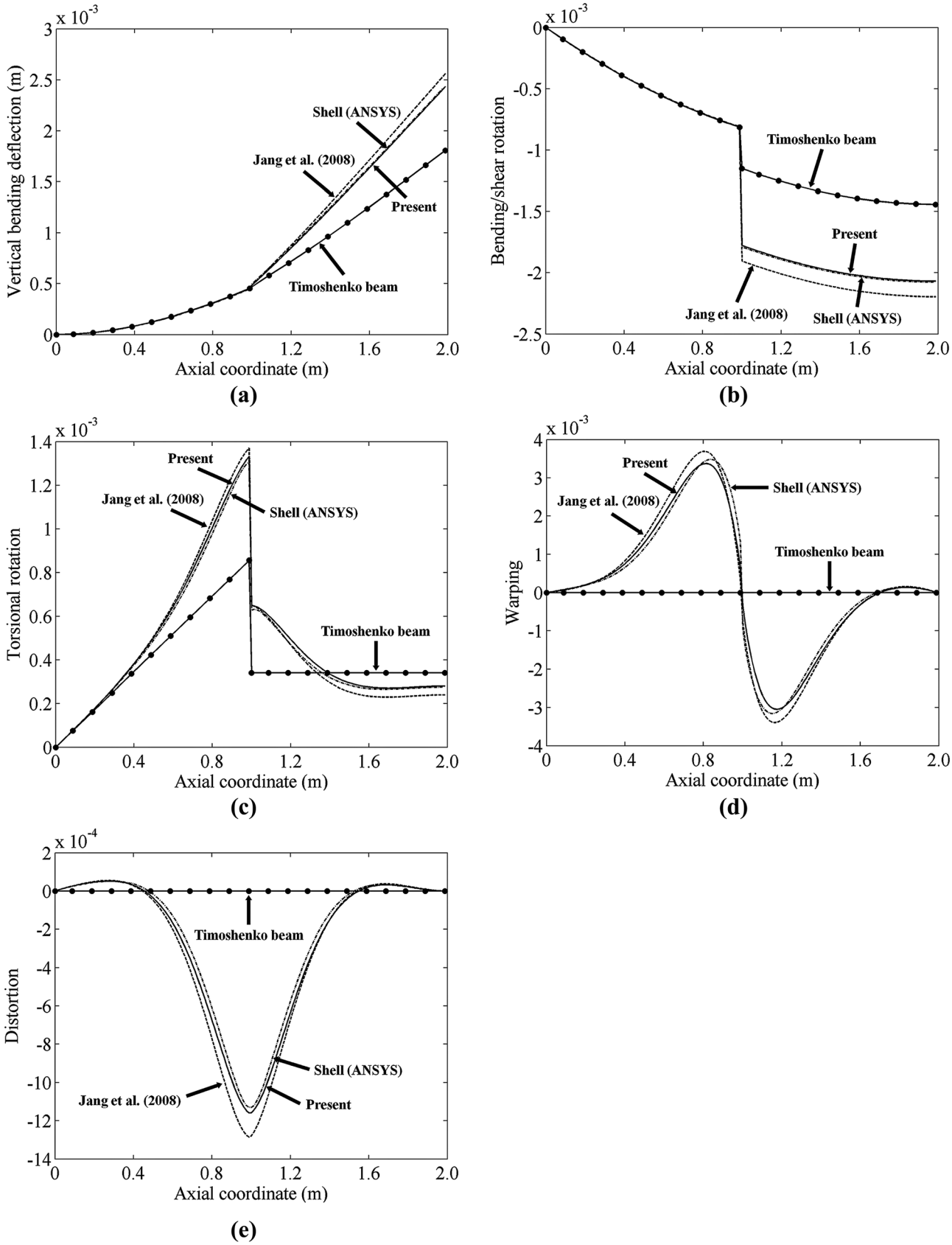

Fig. 6 Numerical results for the two-beam structure in Fig. 1 with $b = 50$ mm, $h = 100$ mm, $\phi = 30$ deg: (*a*) vertical bending deflection V, (*b*) bending/shear rotation β, (*c*) torsional rotation θ, (*d*) warping U, and (*e*) distortion χ

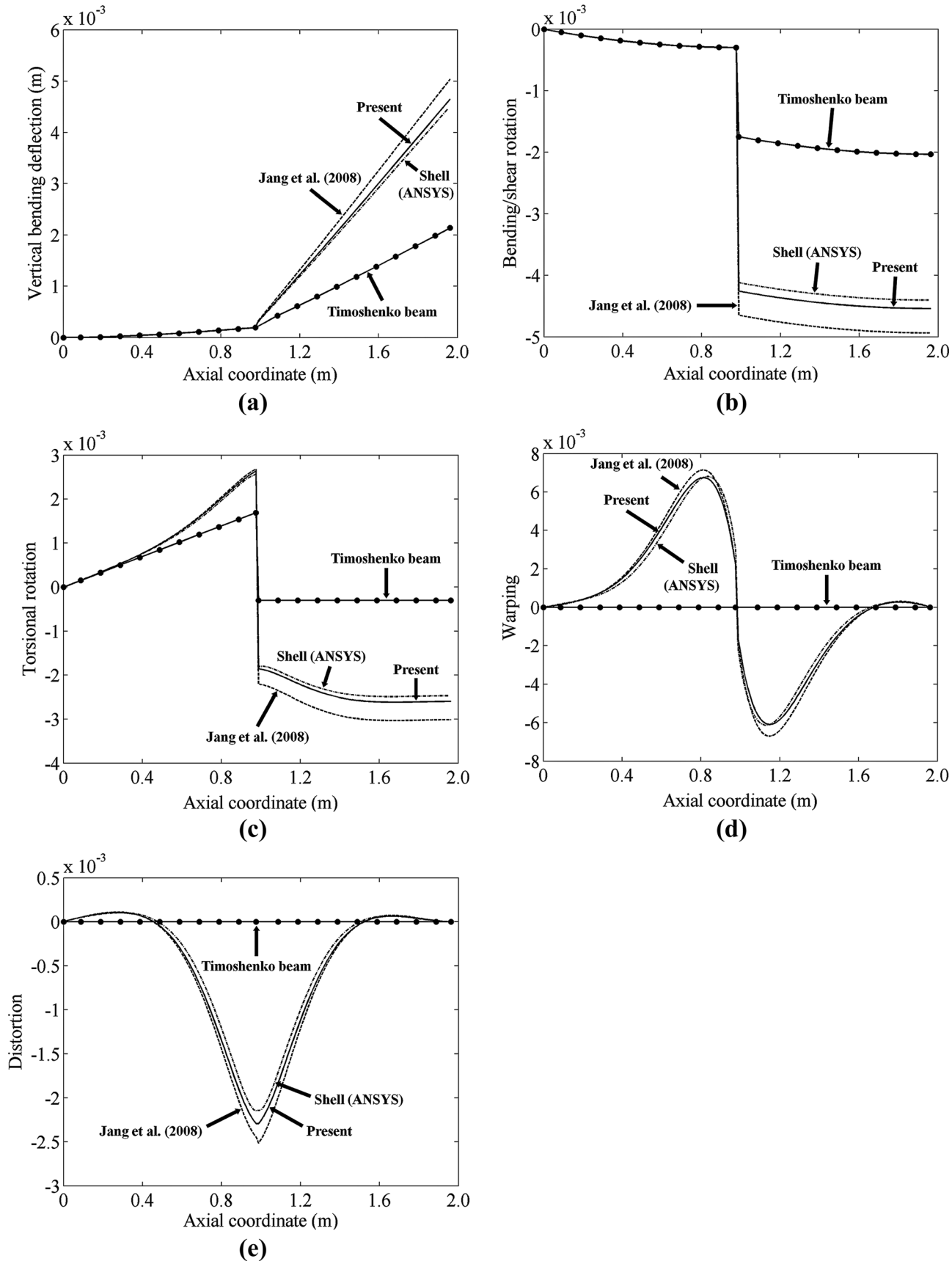

Fig. 7 Numerical results for the two-beam structure in Fig. 1 with $b = 50$ mm, $h = 100$ mm, $\phi = 90$ deg: (*a*) vertical bending deflection V, (*b*) bending/shear rotation β, (*c*) torsional rotation θ, (*d*) warping U, and (*e*) distortion χ

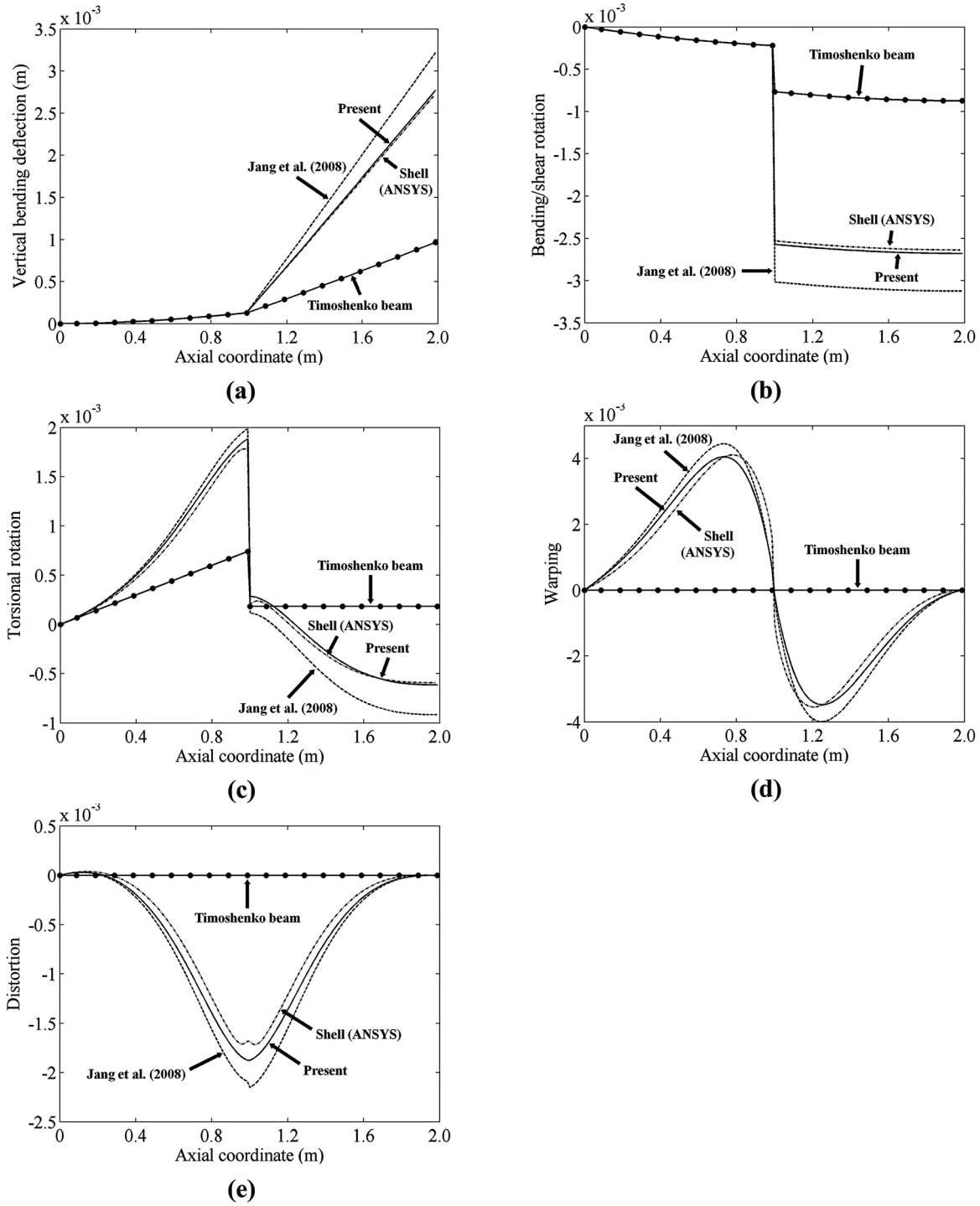

Fig. 8 Numerical results for the two-beam structure in Fig. 1 with $b = 50$ mm, $h = 150$ mm, $\phi = 60$ deg: (*a*) vertical bending deflection V, (*b*) bending/shear rotation β, (*c*) torsional rotation θ, (*d*) warping U, and (*e*) distortion χ

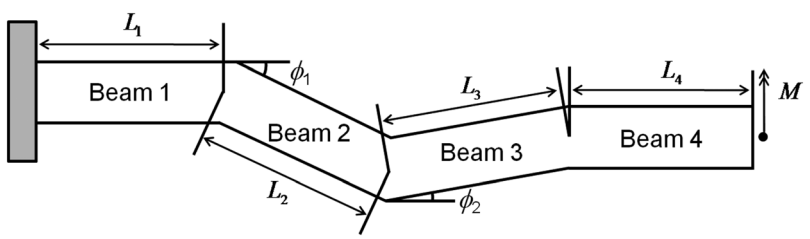

Fig. 9 A thin-walled beam structure having three angled joints under a bending moment M ($L_1 = L_2 = L_3 = L_4 = 1000$ mm, $\phi_1 = -45$ deg, $\phi_2 = 20$ deg, $M = -100$ Nm)

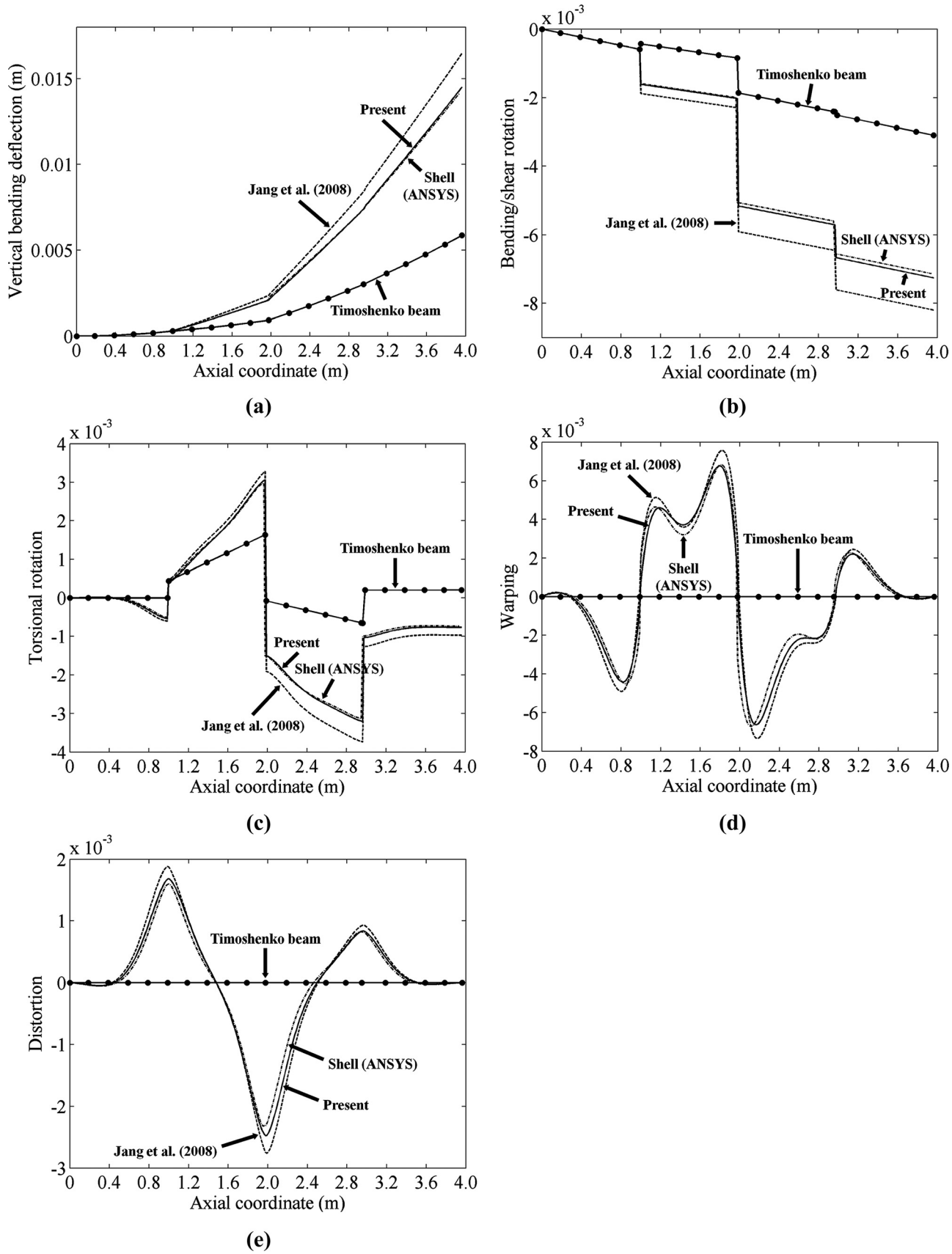

Fig. 10 Numerical results for the beam structure shown in Fig. 9: (*a*) vertical bending deflection *V*, (*b*) bending/shear rotation β, (*c*) torsional rotation θ, (*d*) warping *U*, and (e) distortion χ

$$\mathbf{T}(\phi)\cdot\mathbf{T}(-\phi)=\begin{bmatrix}1&0&0&0&0\\0&1&0&0&0\\0&0&1&\frac{2b}{b+h}t_{54}(t_{44}+t_{55})&\frac{2b}{b+h}(t_{55}^2+t_{54}t_{45}-1)\\0&0&0&t_{44}^2+t_{45}t_{54}&t_{45}(t_{44}+t_{55})\\0&0&0&t_{54}(t_{44}+t_{55})&t_{55}^2+t_{45}t_{54}\end{bmatrix}$$
$$\equiv\begin{bmatrix}1&0&0&0&0\\0&1&0&0&0\\0&0&1&0&0\\0&0&0&1&0\\0&0&0&0&1\end{bmatrix} \tag{23}$$

From Eq. (23), the following four relations for the undetermined components (t_{44}, etc.) are derived:

$$t_{44}^2+t_{45}t_{54}=1 \tag{24a}$$
$$t_{45}(t_{44}+t_{55})=0 \tag{24b}$$
$$t_{54}(t_{44}+t_{55})=0 \tag{24c}$$
$$t_{55}^2+t_{45}t_{54}=1 \tag{24d}$$

The solutions that satisfy Eq. (24) may not be unique. To deal with this issue, a fundamental multiplication relation valid for any transformation matrix is used as the following proposition, proposition 4.

3.4 Proposition 4: Use of the Relation $\mathbf{T}(\phi)\cdot\mathbf{T}(\phi)=\mathbf{T}(2\phi)$. Finally, we consider another fundamental relation $\mathbf{T}(\phi)\cdot\mathbf{T}(\phi)=\mathbf{T}(2\phi)$. By using Eq. (18), one can write $\mathbf{T}(\phi)\cdot\mathbf{T}(\phi)$ explicitly as

$$\mathbf{T}(\phi)\cdot\mathbf{T}(\phi)=\begin{bmatrix}1&0&0&0&0\\0&\cos(2\phi)&-\sin(2\phi)&0&\frac{2b}{b+h}\sin(2\phi)\\0&\sin(2\phi)&\cos(2\phi)&\frac{2b}{b+h}t_{54}(t_{44}+t_{55})&\frac{2b}{b+h}((t_{55}^2+t_{54}t_{45})-\cos(2\phi))\\0&0&0&t_{44}^2+t_{45}t_{54}&t_{45}(t_{44}+t_{55})\\0&0&0&t_{54}(t_{44}+t_{55})&t_{55}^2+t_{45}t_{54}\end{bmatrix} \tag{25}$$

Observe that the expressions involving t_{44}, t_{45}, t_{54}, and t_{55} in Eq. (25) are exactly the same as those derived as Eq. (24) from proposition 3. Therefore, one can finally express $\mathbf{T}(2\phi)=\mathbf{T}(\phi)\cdot\mathbf{T}(\phi)$ as, without any unknowns,

$$\mathbf{T}(2\phi)=\begin{bmatrix}1&0&0&0&0\\0&\cos(2\phi)&-\sin(2\phi)&0&\frac{2b}{b+h}\sin(2\phi)\\0&\sin(2\phi)&\cos(2\phi)&0&\frac{2b}{b+h}(1-\cos(2\phi))\\0&0&0&1&0\\0&0&0&0&1\end{bmatrix} \tag{26}$$

Putting ϕ instead of 2ϕ in Eq. (26) yields the exact expression of $\mathbf{T}(\phi)$ such that

$$\begin{Bmatrix}V\\\beta\\\theta\\U\\\chi\end{Bmatrix}_2=\mathbf{T}(\phi)\begin{Bmatrix}V\\\beta\\\theta\\U\\\chi\end{Bmatrix}_1$$
$$=\begin{bmatrix}1&0&0&0&0\\0&\cos\phi&-\sin\phi&0&\frac{2b}{b+h}\sin\phi\\0&\sin\phi&\cos\phi&0&\frac{2b}{b+h}(1-\cos\phi)\\0&0&0&1&0\\0&0&0&0&1\end{bmatrix}\begin{Bmatrix}V\\\beta\\\theta\\U\\\chi\end{Bmatrix}_1 \tag{27}$$

Equation (27) shows that the distortion (χ_1) of beam 1 affects the bending/shear rotation (β_2) and torsional rotation (θ_2) of beam 2 at the joint. On the other hand, the warping ($\mathbf{U}_1$) of beam 1 is not coupled with any other deformation but is directly transmitted only to the warping ($\mathbf{U}_2$) of beam 2. Although the final form of the transformation matrix $\mathbf{T}$ of the thin-walled box beam theory is simple and compact, the exact derivation is given here for the first time.

4 Numerical Examples

Two case studies, considered earlier by Jang et al. [19], will be performed to demonstrate the accuracy and validity of the derived transformation $\mathbf{T}$. The present $\mathbf{T}$ matrix will be used in the one-dimensional finite element method employing the five kinematic variables. Since the higher-order box beam finite element implementation is a standard procedure, the detailed steps to obtain the numerical results will be omitted.

4.1 Case Study 1: Two Box Beams Connected at an Angled Joint. As the first case study, the beam structures shown in Fig. 1 are analyzed for various joint angles ϕ and aspect ratios of the cross section. Some of the beam dimensions are fixed to be $t=2$ mm and $L=1000$ mm, and the material properties are E (Young's modulus) $=200$ GPa and ν (Poisson's ratio) $=0.3$. The one end of the structure is clamped and the other end, denoted as C, is subjected to a vertical force $P=100$ N. The cross section C is assumed to be rigid (no warping or distortion).To check the accuracy of the present approach using the derived $\mathbf{T}$ matrix, the displacements obtained by the proposed approach are compared with those by ANSYS shell elements [20]. The results are also compared with those based on the same higher-order beam theory incorporating the joint-displacement minimization technique (Jang et al. [19]). Also, the displacements by the standard Timoshenko beam elements are plotted for comparison.

Figure 5 shows the axial distributions of the five field variables for the case of $b=50$ mm, $h=100$ mm, and $\phi=60$ deg. The numbers of the discretizing finite elements are 60 for the present beam analysis and 3960 for the shell analysis. In Fig. 5, the results by the present approach are virtually identical to those by the shell calculation while the Timoshenko beam results are quite off from

the shell results. Two-beam structures having different joint angles were also investigated and the numerical results are plotted in Figs. 6 and 7. The responses of the field variables for different aspect ratios of the cross section, $b = 50$ mm and $h = 150$ mm are also illustrated in Fig. 8. The results by the present approach agree well with the shell element results compared with the results by the Timoshenko theory and those by Jang et al. [19]. Although not presented here, the present approach was shown to produce accurate results for box beams of different aspect ratios with various joint angles.

4.2 Case Study 2: Four Box Beams Serially Connected at Angled Joints. Figure 9 illustrates a structure of four thin-walled box beams connected at three joints. The dimensions of the cross sections of all beams are $b = 50$ mm, $h = 100$ mm, and $t = 2$ mm. The material properties are the same as those in the previous case study. The one end of the structure is clamped while the other end is subjected to a bending moment, $M = 100$ Nm. The cross section of the loaded end is assumed to be rigid. Figure 10 shows that the axial variations of $V, \beta, \theta, U,$ and χ. Unlike the results predicted by the approach by Jang et al. [19] or the Timoshenko beam theory, the present results match the shell finite element results well. The studies with beams of other cross sectional geometries and joint angles also confirmed the superior accuracy of the thin-walled beam analysis using the exact transformation derived in the present work.

5 Conclusions

The transformation matrix relating the field variables of a higher-order thin-walled box beam theory at angled joints was derived in an exact form. The proposed conditions to determine unknown elements of the transformation matrix were shown to be sufficient for box beams connected at angled joints that are subject to out-of-plane and torsional loads. With the derived matrix we were able to explain the interaction between the field variables of the two beams connected at an angle joint. Specifically, the distortion of one beam is coupled with the bending/shear and torsional rotations of the other while the warping deformation of one beams is not coupled with other field variables of the other beam but only with the warping deformation of the other beam. The present derivation of the joint matching condition is expected to serve as an important building block to expedite the research on higher-order beam theories for arbitrarily shaped, connected thin-walled beams.

Acknowledgment

The first and third authors were supported by the National Research Foundation of Korea (NRF) (Grant No. 2011-0017445) funded by the Korean Ministry of Education, Science and Technology (MEST) contracted through IAMD at Seoul National University and WCU program (No. R31-2010-000-10083-0) through NRF funded by MEST. The second author was supported by the National Research Foundation of Korea (Grant No. 2010-0023472).

Appendix

The section shape functions ψ are explicitly given. The index j indicates the edge number of the beam cross section.

$$\psi_n^V(s_j) = 0 \ (j = 1,3) \quad \text{and} \quad (-1)^{(j-2)/2} (j = 2,4) \tag{A1}$$

$$\psi_s^V(s_j) = (-1)^{(j-1)/2} (j = 1,3) \quad \text{and} \quad 0 \ (j = 2,4) \tag{A2}$$

$$\psi_z^V(s_j) = 0 \tag{A3}$$

$$\psi_n^\beta(s_j) = 0 \tag{A4}$$

$$\psi_s^\beta(s_j) = 0 \tag{A5}$$

$$\psi_z^\beta(s_j) = (-1)^{(j-1)/2} \mathrm{s}_i \ (j = 1,3) \quad \text{and} \quad (-1)^{(j-2)/2} \frac{h}{2} (j = 2,4) \tag{A6}$$

$$\psi_n^\theta(s_j) = -s_j \tag{A7}$$

$$\psi_s^\theta(s_j) = \frac{b}{2} (j = 1,3) \quad \text{and} \quad \frac{h}{2} (j = 2,4) \tag{A8}$$

$$\psi_z^\theta(s_j) = 0 \tag{A9}$$

$$\psi_n^U(s_j) = 0 \tag{A10}$$

$$\psi_s^U(s_j) = 0 \tag{A11}$$

$$\psi_z^U(s_j) = \frac{b}{2} s_j \ (j = 1,3) \quad \text{and} \quad -\frac{h}{2} s_j \ (j = 2,4) \tag{A12}$$

$$\psi_n^\chi(s_j) = -\frac{4}{h(b+h)} s_j^3 + \frac{2b+h}{b+h} s_j \ (j = 1,3) \quad \text{and} \quad + \frac{4}{b(b+h)} s_j^3 - \frac{b+2h}{b+h} s_j \ (j = 2,4) \tag{A13}$$

$$\psi_s^\chi(s_j) = \frac{bh}{b+h} (j = 1,3) \quad \text{and} \quad -\frac{bh}{b+h} (j = 2,4) \tag{A14}$$

$$\psi_z^\chi(s_j) = 0 \tag{A15}$$

where

$$-\frac{h}{2} \le s_1, s_3 \le \frac{h}{2} \quad \text{and} \quad -\frac{b}{2} \le s_2, s_4 \le \frac{b}{2}$$

References

[1] Vlasov, V. Z., 1961, *Thin Walled Elastic Beams*, Israel Program for Scientific Translations, Jerusalem.

[2] Bazant, Z., and El Nimeiri, M., 1974, "Stiffness Method for Curved Box Girders at Initial Stress," ASCE J. Struct. Div., **100**(10), pp. 2071–2090. Available at: http://cedb.asce.org/cgi/WWWdisplay.cgi?22132

[3] Mikkola, M. J., and Paavola, J., 1980, "Finite Element Analysis of Box Girders," ASCE J. Struct. Div., **106**(6), pp. 1343–1357. Available at: http://cedb.asce.org/cgi/WWWdisplay.cgi?5015498

[4] Boswell, L. F., and Zhang, S. H., 1983, "A Box Beam Finite Element for the Elastic Analysis of Thin-Walled Structures," Thin-Walled Struct., **1**(4), pp. 353–383.

[5] Maisel, B. I., 1982, *Analysis of Concrete Box Beams Using Small-Computer Capacity*, Cement and Concrete Association, London.

[6] Zhang, S. H., and Lyons, L. P. R., 1984, "A Thin-Walled Box Beam Finite Element for Curved Bridge Analysis," Comput. Struct., **18**(6), pp. 1035–1046.

[7] Balch, C. D., and Steele, C. R., 1987, "Asymptotic Solutions for Warping and Distortion of Thin-Walled Box Beams," J. Appl. Mech., **54**(1), pp. 165–173.

[8] Razaqpur, A. G., and Li, H. G., 1991, "A Finite Element with Exact Shape Functions for Shear Lag Analysis in Multi-Cell Box Girders," Comput. Struct., **39**(1-2), pp. 155–163.

[9] Boswell, L. F., and Li, Q., 1995, "Consideration of the Relationships Between Torsion, Distortion and Warping of Thin-Walled Beams," Thin-Walled Struct., **21**(2), pp. 147–161.

[10] Kim, J. H., and Kim, Y. Y., 1999, "Analysis of Thin-Walled Closed Beams With General Quadrilateral Cross Sections," J. Appl. Mech., **66**(4), pp. 904–912.

[11] Kim, J. H., and Kim, Y. Y., 2001, "Thin-Walled Multicell Beam Analysis for Coupled Torsion, Distortion, and Warping Deformations," J. Appl. Mech., **68**(2), pp. 260–269.

[12] Sumami, Y., Yugawa, T., and Yoshida, Y., 1988, "Analysis of Joint Rigidity of In-Plane Bending of Plane-Joint Structures," JSAE Rev., **9**(2), pp. 44–51.

[13] Sunami, Y., Yugawa, T., and Yoshida, Y., 1990, "Analysis of the Joint Rigidity of the Automotive Body Structure-Out-of-Plane Bending of Plane-Joint Structures," JSAE Rev., **11**(3), pp. 59–66. Available at: http://www.bookpark.ne.jp/cm/jsae/search_e.asp?page=3&table=JSAQ&bk_title=&bk_author=&bk_comment=&bk_company=&keyword=Sunami+Y&condition=and&bk_dateS=&bk_dateE=&option1=&option2=&option3=&content_id=&category=

[14] Lee, K., and Nikolaidis, E., 1992, "A Two-Dimensional Model for Joints in Vehicle Structures," Comput. Struct., **45**(4), pp. 775–784.

[15] Garro, L., and Vullo, V., 1986, "Deformations Car Body Joints Under Operating Conditions," SAE, pp. 5403–5420.

[16] El-Sayed, M. E. M., 1989, "Calculation of Joint Spring Rates Using Finite Element Formulation," Comput. Struct., **33**(4), pp. 977–981.

[17] Jang, G. W., Kim, K. J., and Kim, Y. Y., 2008, "Higher Order Beam Analysis of Box Beams Connected at Angled Joints Subject to Out of Plane Bending and Torsion," Int. J. Numer. Methods Eng., **75**(11), pp. 1361–1384.

[18] Jang, G. W., and Kim, Y. Y., 2009, "Higher-Order In-Plane Bending Analysis of Box Beams Connected at an Angled Joint Considering Cross-Sectional Bending Warping and Distortion," Thin-Walled Struct., **47**(12), pp. 1478–1489.

[19] Jang, G. W., and Kim, Y. Y., 2009, "Vibration Analysis of Piecewise Straight Thin-Walled Box Beams Without Using Artificial Joint Springs," J. Sound Vib., **326**(3-5), pp. 647–670.

[20] ANSYS, 2007, *ANSYS Structural Analysis Guide*.